applied sciences

MDPI

Article

Binary Mixes of Self-Compacting Concrete with Municipal Solid Waste Incinerator Bottom Ash

Joel R. Simões [1], Pedro R. da Silva [1,2] and Rui V. Silva [2,*]

[1] Instituto Superior de Engenharia de Lisboa, Instituto Politécnico de Lisboa, R. Conselheiro Emídio Navarro 1, 1959-007 Lisboa, Portugal; A38064@alunos.isel.pt (J.R.S.); silvapm@dec.isel.pt (P.R.d.S.)
[2] CERIS, Instituto Superior Técnico, Universidade de Lisboa, Av. Rovisco Pais, 1049-001 Lisboa, Portugal
* Correspondence: rui.v.silva@tecnico.ulisboa.pt

Abstract: With the objective of establishing a viable alternative to the use of cement, the main objective of this study is to verify the possibility of using municipal solid waste incinerator bottom ash (MIBA) as a partial cement replacement, thereby reducing the environmental impact associated with the use of concrete as a building material. To this end, self-compacting concrete (SCC) binary mixes of cement and MIBA were evaluated in their fresh and hardened state (i.e., self-compactability, mechanical and durability related performance). Four SCC mixes were produced to cover a wide range of replacement levels of cement with MIBA, namely: 20%, 30%, 40% and 50%. A fifth SCC mix, without MIBA, was produced with 30% fly ash to carry out a comparative analysis with composites with well-established performance. The results showed that the use of bottom ash from municipal solid waste incinerators caused an overall decline in the performance of self-compacting concrete. Apart from the smaller number of reactive phases in the bottom ash when compared with fly ash, which led to a slower rate of strength development, the decline was also caused by the increased porosity from the oxidation of aluminium particles. Nevertheless, the results showed promising indicators regarding the durability of mixes with 20% MIBA, with values very similar to those of reference concrete.

Keywords: self-compacting concrete; municipal solid waste; incineration; bottom ash; fresh properties; mechanical properties; durability

Citation: Simões, J.R.; Silva, P.R.d.; Silva, R.V. Binary Mixes of Self-Compacting Concrete with Municipal Solid Waste Incinerator Bottom Ash. *Appl. Sci.* **2021**, *11*, 6396. https://doi.org/10.3390/app11146396

Academic Editor: Giuseppe Lacidogna

Received: 14 June 2021
Accepted: 7 July 2021
Published: 11 July 2021

1. Introduction

The concentration of CO_2 in the atmosphere has been increasing progressively, with reported values of increase from 324 ppm in 1969 to 415 ppm in 2020 alone [1]. According to experts, to avoid climate change in the second half of the 21st century, CO_2 emissions must be reduced by 90% by 2030 [2]. Today, the World's annual concrete production is approximately 1×10^{10} tonnes. This results in large amounts of CO_2 emissions mainly due to the production of Portland cement. This binder currently accounts for 74–81% of the total CO_2 emissions of concrete manufacture [3]. The production of one tonne of Portland cement emits about 0.94 tons of CO_2 and the cement industry is responsible for about 8% of all CO_2 emissions from all economic sectors [4]. It is estimated that 1.5 to 1.7 tons of natural resources are used as raw material per tonne of Portland cement [5]. Given the current status, there is an urgent need to change the methods and principles of Portland cement manufacturing and to evaluate in detail the use of various industrial wastes as cement replacement in the production of cementitious composites. The use of certain wastes, such as municipal solid waste incinerator bottom ash (MIBA), can prevent the excessive consumption of natural resources, is capable of reducing energy expenditure, can reduce the cement and/or concrete cost of manufacturing and can be beneficial for the environment due to the reduction of air pollution, landfill space, among other environmental impacts [6,7].

In addition to the problem of CO_2 emissions into the atmosphere, the production of municipal solid waste is also expected to increase by approximately 2.2 billion tonnes per year by 2025 [8], which will consequently lead to an increase in by-products resulting from their combustion. In waste management policies, the priority is to prevent the production of waste; however, when this does not happen, the next steps include recycling, recovery, incineration and, as a last resort, the landfilling of wastes. Due to the scarcity of space available for the disposal of waste in landfills, the costs of this process tend to increase, which, together with issues like water contamination and public health, strengthen the need to find more technically, economically and environmentally friendly solutions.

Currently, MIBA is commonly used for the construction of unbound layers for road pavements [9]. However, to respond to the demand for new materials that minimize the environmental impact of the construction sector, some studies have been developed to validate the use of MIBA in the production of concrete [7]. These have essentially focused on the mechanical behaviour of composites using MIBA as cement replacement. Amat et al. [10] expressed the possibility of MIBA having pozzolanic or hydraulic behaviour due to their composition being similar to that of cement, but observed a decrease in compressive strength with the increase of MIBA in concrete. Other researchers found a similar decline in performance with increasing replacement levels [11–13]. Simões et al. [14] used MIBA in combination with fly ash and cement in the production of ternary self-compacting concrete mixes; despite the decline in performance with increasing MIBA content, all mixes demonstrated adequate levels of workability according with existing regulations. Promising results are likely to be observed in mixes with relatively high replacement levels if MIBA is adequately treated before use. A pre-drying and milling process is fundamental to achieve a particle size distribution close to that of cement. There are few (and little in-depth) studies on, for example, its durability. Therefore, it is clear that there is a need for further studies on the incorporation of these ashes in cementitious composites.

This study belongs to a state-funded research project, the mission of which is to further valorise MIBA in new building materials, thereby reducing the environmental impacts of the waste management and construction sectors. The main objective of the present work is to evaluate the properties of binary mixes of self-compacting concrete (SCC) with cement and MIBA in the fresh and hardened state, to verify the applicability of this addition in the production of concrete. Different combinations in mix design were tried (i.e., 0%, 20%, 30%, 40% and 50% of MIBA instead of cement). The requirements in the fresh state were evaluated based on fluidity, viscosity, filling capacity and flowability in accordance with current standards. The tests in the hardened state were divided into two main groups (i.e., mechanical and durability-related performance). Mechanical properties included uniaxial compressive strength in cubic and cylindrical specimens, splitting tensile strength, modulus of elasticity and shrinkage. Durability properties included the evaluation of open porosity through the water absorption by immersion and by capillary action tests, chloride ion penetration, electrical resistivity and carbonation. The ultrasonic pulse velocity test was also carried out to evaluate the specimens' densification.

2. Materials and Methods

2.1. Cement, MIBA and Fly Ash

Portland cement CEM I 42.5 R, according to EN 197-1 [15], was used. This cement consists essentially of clinker (greater than 95%), with minimum values of 2-day and 28-day compressive strength of 20 MPa and 42.5 MPa, respectively. Two mineral additions were used as cement replacement: fly ash (FA), used to produce the reference concrete (RC), according to EN 450-1 [16] and bottom ash resulting from the municipal solid waste incinerator (MIBA) for the remaining mixtures.

2.2. Aggregates

Four different types of aggregates were used: two types of siliceous sand (fine sand 0/2 and coarse sand 0/4) and two types of limestone gravel (gravel 1 and gravel 2). For

the characterization of the aggregates, their density, water absorption and particle size distribution were evaluated according to EN 12620: 2002+A1 [17].

2.3. Water-Reducing Admixture and Water

Tap water complying with EN 1008 [18] was used. A third-generation high-range water-reducing admixture (S_p) complying with EN 934-1 [19] and EN 934-2 [20] was used.

2.4. Mix Design

Different proportions of cement replacement were used for this study. First, a reference concrete (RC) with fly ash (FA) content of 30% was produced. Four self-compacting mixes were produced with 20%, 30%, 40% and 50% MIBA as cement replacement. Hereon, these mixes will be referred to as RC, C20BA, C30BA, C40BA and C50BA, respectively.

The mixes' composition (Table 1) was based on the method proposed by Nepomuceno et al. [21] and Silva et al. [22]. The volumetric ratio between the fine materials (i.e., volume of cement and additions—V_p) and fine aggregates (total volume of sand 0/2 and 0/4—V_s) was fixed at $V_p/V_s = 0.80$. The volume of voids, V_V, was considered constant and equal to 0.03 m^3, and the volumetric ratio of the mortar content (V_m) and coarse aggregate (V_g) was $V_m/V_g = 2.275$. The aforementioned ratios were maintained for all mixes. The volumetric ratio between water (volume of water—V_w) and the fine materials for the RC was $V_w/V_p = 0.8$. However, mixes C20BA, C30BA, C40BA and C50BA had $V_w/V_p = 1.0$, which meant that the RC mix had a w/c of 0.36 and mixes containing MIBA of 0.41. The mass ratio of superplasticizer (Sp) to fine material (P) of the RC and the mixes containing MIBA was of $Sp/P_{\%} = 0.75$ and $S_p/P_{\%} = 1.00$, respectively.

Table 1. Concrete mix proportions.

Mix Proportions (kg/m^3)	RC	C20BA	C30BA	C40BA	C50BA
Cement	482	496	452	387	323
FA	151	-	-	-	-
MIBA	-	99	154	206	257
S_p	4.8	5.9	6	5.9	5.8
Water	176	197	206	206	206
Fine aggregate $_{0/2}$	354	318	332	332	332
Fine aggregate $_{0/4}$	350	314	328	328	328
Coarse aggregate $_1$	384	419	384	384	384
Coarse aggregate $_2$	391	427	391	391	391

2.5. Test Methods and Sample Preparation

X-ray fluorescence (XRF) was used to determine the oxide chemical composition of cement, FA and MIBA. X-ray diffraction (XRD) was used to identify the crystalline phases. Scanning electron microscopy (SEM), energy-dispersive X-ray spectroscopy (EDS) and metallic aluminium quantification were also carried out. The consumption of calcium oxide (CaO) per gram was carried out by Chapelle test to determine the pozzolanic activity of MIBA and FA [23,24].

The SCC mixes' workability was evaluated using the slump-flow test [25]. A V-funnel test was also performed to identify the viscosity and filling capacity [26]. Flowability was ascertained with the L-box flow test [27].

Specimens subjected to compressive and splitting tensile strength, secant modulus of elasticity and water absorption by immersion tests were cured in water at 20 ± 2 °C until testing age. Shrinkage specimens were placed in a dry chamber at 20 ± 2 °C and 50% ± 5% relative humidity immediately after demoulding and remained there throughout the test. Specimens subjected to the water absorption by capillary action test were cured in water at 20 ± 2 °C for 14 days and then placed in a chamber at 40 ± 5 °C for an additional 14 days until testing age. The curing regimen for specimens subjected to carbonation was

the same as the previous ones for the first 14 days and, after that, were sectioned into smaller specimens and subsequently coated with an acrylic resin in both extremities. The specimens were then placed in a dry chamber at 20 ± 2 °C and 50% ± 5% relative humidity for another 14 days. After these 28 days, the specimens were placed in an accelerated carbonation chamber at 23 ± 3 °C, with relative humidity between 55% and 65% and with a CO_2 content of 5 ± 0.1%. Chloride ion penetration test specimens were cured in water for 21 days before being sectioned into smaller specimens. After that, they were placed in the dry chamber until testing age.

Compressive strength was evaluated in 150-mm cube specimens after 7, 28 and 91 days, and in 150-mm diameter and 300-mm high cylindrical specimens after 28 and 91 days according to EN 12390-3 [28]. The splitting tensile strength and secant modulus of elasticity were also determined on cylindrical specimens as described in EN 12390-6 [29] and LNEC E 397 [30], respectively, after 28 and 91 days.

The quality of the concrete mixes was determined by means of the ultrasonic pulse velocity test, according to EN 12504-4 [31]. The shrinkage test of the SCC samples was tested on 100 × 100 × 400 mm prisms specimens according to LNEC E 398 [32].

Accelerated carbonation (LNEC E 391 [33]), water absorption by immersion (LNEC E 394 [34]), chloride ion penetration (LNEC E 463 [35]) and electrical resistivity tests (Luping [36]) tests were carried out to evaluate the durability of mixes.

3. Results and Discussion

3.1. Characterization of the Materials

The results of the modified Chapelle test, by titration with 0.1M hydrochloric acid, determined the content of unconsumed $Ca(OH)_2$ (free content), which were meant to react with the reactive aluminosilicate phases present in the FA and MIBA, during 16 h at 90 ± 5 °C. Two grams of CaO laboratory-grade and one gram of the by-product diluted in distilled water were used in this reaction. The reactions presented in the titration are the following:

$$CaO + 2HCl \rightarrow CaCl_2 + H_2O \quad (1)$$

$$Ca(OH)_2 + 2HCl \rightarrow CaCl_2 + 2H_2 \quad (2)$$

Through Equation (3), it is possible to calculate the mg of Ca $(OH)_2$/g of by-product.

$$(\text{mg } Ca(OH)_2)/(\text{g by-product}) = (28 \times (v_3 - v_2) \times F_c)/(m_2) \times 1.32 \quad (3)$$

where m_2 is the mass (g) of the pozzolanic material, v_2 the volume of HCl consumed by the sample; v_3 the volume of HCl consumed by the blank; F_c, the correction factor for a 0.1 M solution and 1.32 the molecular relationship between Ca $(OH)_2$/CaO. Values of 566 mg and 445 mg of $Ca(OH)_2$ per g of residue for FA and MIBA were respectively obtained. Materials with results higher than 436 mg $Ca(OH)_2$/g of addition [37] can be considered as pozzolanic, which is the case for both additions.

Table 2 presents the XRF characterization for cement, FA and MIBA. The results show that the cement complies with EN 197-1 [15]. According to EN 450-1 [16], FA and MIBA can be classified as category B, with respect to the loss on ignition. However, only the FA met the required sum of aluminium, iron and silicon oxides, exceeding the minimum value established by the norm (i.e., 70%). According to ASTM C618-19 [38], MIBA could be classified as Class C fly ash.

Table 2. Chemical characterization for cement, FA and MIBA (% by mass).

Materials	Al_2O_3	CaO	Fe_2O_3	K_2O	MgO	Na_2O	SiO_2	SO_3	Cl-	IR	LOI
CEM I (%)	5.24	62.7	3.17	-	2.23	-	19.6	3.13	0.01	1.37	2.94
Fly ash (%)	24.7	2.63	5.40	1.11	1.01	0.89	54.7	1.38	<0.01	-	5.10
MIBA (%)	4.10	23.0	9.21	1.57	2.37	2.40	51.8	2.42	0.70	-	2.40

The XRD of MIBA is presented in Figure 1. The main crystalline phases present correspond to quartz (SiO_2) and calcite ($CaCO_3$).

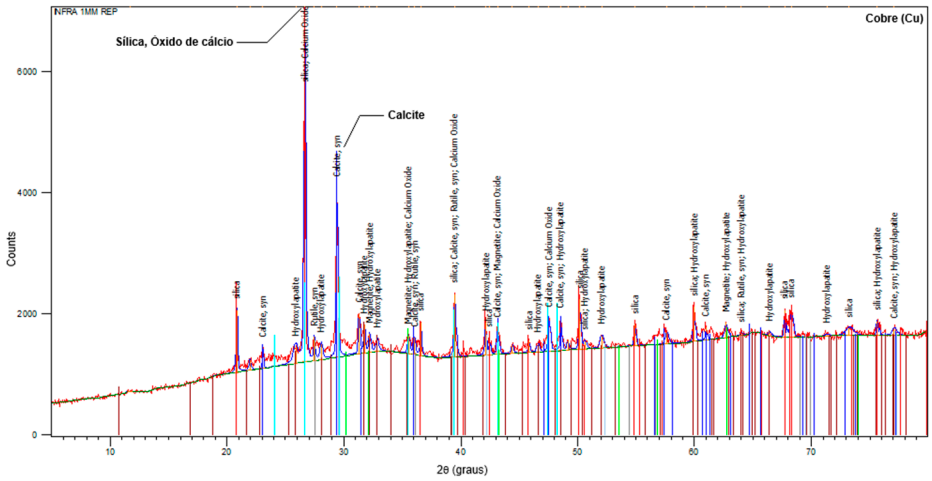

Figure 1. XRD pattern for MIBA.

The morphology of MIBA can be observed in Figure 2. Most of the particles have a porous microstructure and angular shape, which potentially translates into a greater amount of water required to cover the particles and achieve the desired workability. Likewise, the results of the EDS test are presented, where it is observed that the element found in the highest proportion is oxygen with 23.3%, followed by calcium with 15.2%, 8.7% for silicon, 6.63% of aluminium (Al) and 4.1% of iron.

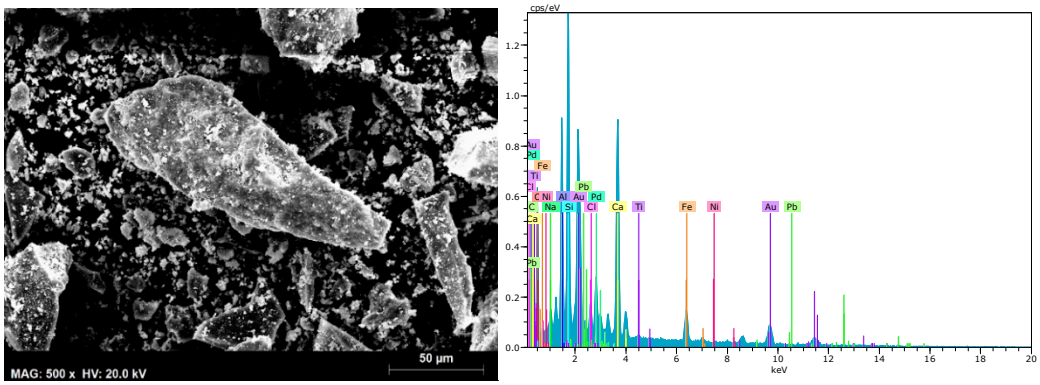

Figure 2. SEM (**left**) and EDS (**right**) of MIBA.

The quantification of metallic aluminium in MIBA was possible by means of the stoichiometry of the reaction between the metal and the OH^- from the NaOH added to the solution. The volume of released hydrogen gas was measured and converted to its corresponding mass. The results showed that 6.3 L of H_2 were released for each kg of MIBA, which meant that there were 4.36 g of Al for each kg of MIBA.

3.2. Properties of Aggregates

Two siliceous sands were used, sand 0/4, with a specific gravity of 2.5 g/cm^3, fineness modulus of 3.28 and water absorption of 1.30%, and sand 0/2, with a specific gravity of 2.5 g/cm^3, fineness modulus of 2.04 and water absorption of 0.75%. Two types of coarse aggregates were used, gravel 1, with a rodded-dry density of 2.5 g/cm^3, D_{max} of 11.2 mm and water absorption of 1.46%, and gravel 2, with a specific gravity of 2.6 g/cm^3, D_{max} of 16 mm and water absorption of 0.78%. Table 3 shows the aggregates' particle size distribution.

Table 3. Particle size distribution of natural aggregates.

Sive Size (mm)	Cumulative Pass Amount (%)			
	Fine Aggregate		Coarse Aggregate	
	Sand 0/2	Sand 0/4	Gravel 1	Gravel 2
22.4	100.0	100.0	100.0	100.0
16	100.0	100.0	100.0	83.4
11.2	100.0	100.0	80.1	30.0
8	100.0	100.0	39.2	4.4
5.6	100.0	99.5	5.7	2.6
4	100.0	98.2	1.2	1.6
2	99.9	89.1	0.7	1.3
1	99.4	59.4	0.5	0.9
0.5	80.7	21.5	0.5	0.5
0.25	16.1	3.5	0.4	0.3
0.125	0.3	0.3	0.2	0.1
0.063	0.0	0.0	0.0	0.0
Fineness modulus	2.04	3.28	6.57	7.08

3.3. Fresh State Performance

The results of the slump-flow, funnel and L-box tests inferred that the concrete mixes were self-compacting. All mixes were classified as VS2 (spread time $\geq$ 2.0 s) from the slump-flow test according to EN 206 [39]. The workability of the RC concrete was considered as SF2 (660–750 mm), but mixes containing MIBA were classified as SF1, with slightly less workable mixes. The L-box test results are shown in Table 4. All the mixes were able to pass through the confined spaces and were classified as VF1 according to the funnel test.

Table 4. Fresh concrete properties, slump-flow, V funnel and L box.

Mixes	Slump-Flow		V-Funnel	L Box
	t_{500} (s)	SF (mm)	Tv (s)	PL (H_2/H_1)
RC	2.7	680	5.6	0.9
C20BA	2.7	600	3.6	0.8
C30BA	2.9	645	2.7	0.9
C40BA	3.4	560	2.5	1.0
C50BA	3.7	550	2.2	0.8

Note: t_{500} = flow time; SF = slump flow diameter; Tv = time that the sample takes to fully flow through the V-funnel; PL = passing ability index in the L-box.

3.4. Mechanical Performance

3.4.1. Compressive Strength

Table 5 shows the compressive strength development of cubic ($f_{cm,cube}$) and cylindrical (f_{cm}) specimens. As expected, strength increased over time. However, it decreased with increasing replacement levels of cement with MIBA, as shown in Figure 3. There are several combining factors that led to this decline. Since cement and FA are being directly replaced with a mineral addition with little to no binding ability upon hydration, a strong strength reduction was expected with increasing MIBA contents [10,40]. Moreover, in spite of the pozzolanicity observed in MIBA, it was clearly inferior to that of FA and showed higher content of crystalline phases in the XRD, thereby resulting in slower strength development over time. As mentioned, the water content of MIBA-containing mixes was slightly higher than that of the RC in order to achieve comparable self-compacting behaviour. Naturally, the increase in the water to binder ratio led to a greater porosity of the cementitious microstructure, thus leading to lower strength.

Table 5. Compressive strength in cylindrical at 28 days and 91 days and in cubes at 7 days, 28 days and 91 days.

Mix	7 days		28 days				91 days			
	$f_{cm,cube}$	$\sigma_{fcm,cube}$	$f_{cm,cube}$	$\sigma_{fcm,cube}$	f_{cm}	σ_{fcm}	$f_{cm,cube}$	$\sigma_{fcm,cube}$	f_{cm}	σ_{fcm}
RC	50.3	5.3	57.6	4.2	55.4	12.5	80.1	2.9	65.6	12.4
C20BA	33.7	2.0	35.7	5.5	20.6	0.3	41.3	0.8	22.1	3.7
C30BA	23.9	1.3	24.2	2.5	11.2	0.7	32.6	2.9	15.3	1.4
C40BA	18.1	1.0	21.8	2.1	9.1	0.1	24.8	0.6	10.6	0.7
C50BA	12.9	0.3	16.8	0.8	6.3	0.4	16.0	0.5	6.8	2.1

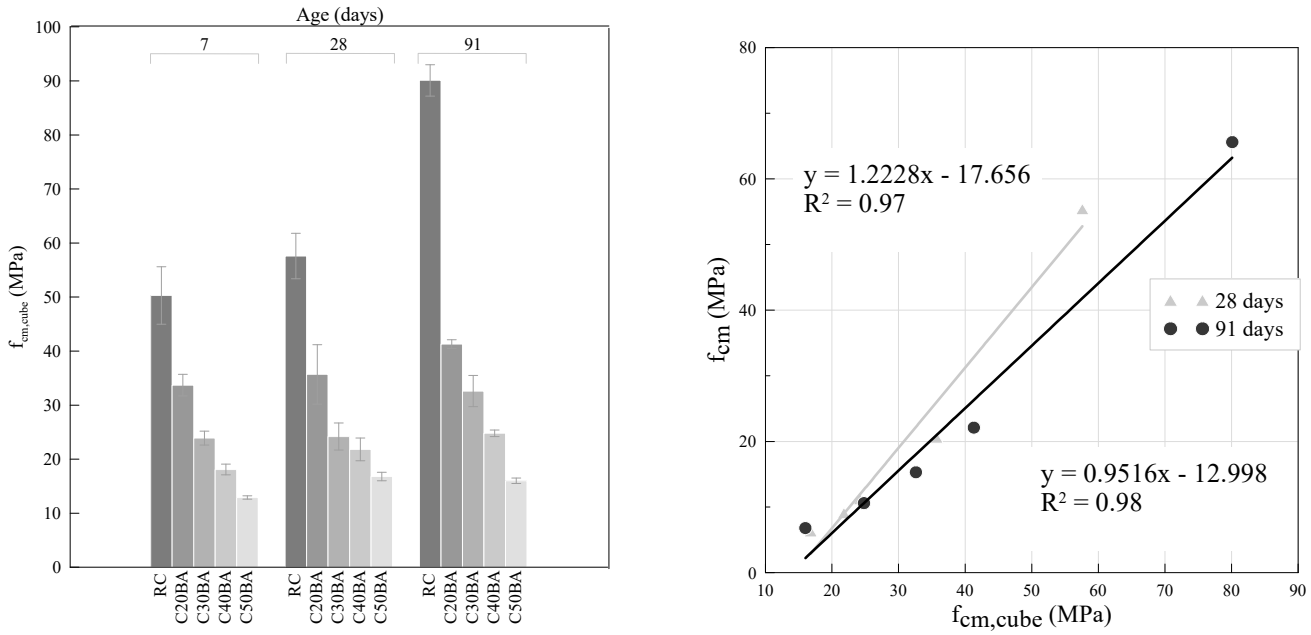

Figure 3. Compressive strength in cubes at 7, 28 and 91 days (**left**); Relationship between compressive strength in cubic and cylindrical specimens at 28 and 91 days (**right**).

Another factor that contributed negatively to the specimens' strength development is the presence of metallic aluminium (Al), the reaction of which with OH^- ions in the mixes' solution generated hydrogen (H_2) in the fresh state, resulting in entrapped gas pockets. This led to an increase in porosity of the MIBA-containing SCC in the hardened state, being one of the main factors of strength decline [41–43]. This inverse proportionality, between MIBA content and compressive strength, had been reported in the study of Simões et al. [14], wherein ternary mixes of SCC were produced with MIBA and FA. The main results showed that the highest percentage of MIBA caused an average compressive strength loss of 74% when compared to the RC. A factor that contributed considerably to this loss was the expansion of specimens from the oxidization of Al particles. Pera et al. [44], when studying the behaviour of concrete with MIBA, also found that the presence of Al led to reduced compressive strength.

Figure 3 also presents the relationship between the average compressive strength in cylindrical and cubic specimens. Little dispersion is observed, and the linear regression presents high correlation coefficients (R^2 = 0.97 after 28 days and R^2 = 0.98 after 91 days).

3.4.2. Splitting Tensile Strength

The splitting tensile strength was carried out on cylindrical specimens after 28 and 91 days, the results of which are shown in Table 6 and Figure 4. This property followed the same trend as that of the compressive strength, i.e., increasing the MIBA content led to a decline in splitting tensile strength, the causes of which are those laid out in the previous section. Furthermore, it is possible that the quality of the interfacial transition zone (ITZ)

may have declined due to the higher MIBA content and increased w/c ratio. Mixes C20BA, C30BA, C40BA and C50BA showed reductions in the 91-day splitting tensile strength of 30%, 52%, 54% and 62%, respectively, when compared to the RC. All specimens practically reached their total splitting tensile strength after 28 days, with coefficients of variation between 2% and 9%. Contrary to that expected, the splitting tensile strength of the RC and C50BA specimens after 91 days was slightly lower than the 28-day splitting tensile strength, thus showing no strength development from the continuous hydration of cement. Li et al. [45], when testing mortars with partial replacement of cement with MIBA (i.e., 0%, 10%, 20%, 30% and 50%), reported a comparable trend concerning the decline in tensile strength with increasing replacement level.

Table 6. Splitting tensile strength versus compressive strength determined according to EC2 at 28 and 91 days.

Mix	$f_{cm,28}$ (MPa)	$f_{ctm,28}$ (MPa)		$f_{cm,91}$ (MPa)	$f_{ctm,91}$ (MPa)	
		EC2	Measured		EC2	Measured
RC	55.4	3.98	5.03	65.6	4.29	4.88
C20BA	20.6	2.37	3.09	22.1	2.48	3.40
C30BA	11.2	1.60	2.32	15.3	1.97	2.36
C40BA	9.10	1.37	2.19	10.6	1.53	2.24
C50BA	6.28	1.03	1.96	6.85	1.11	1.87

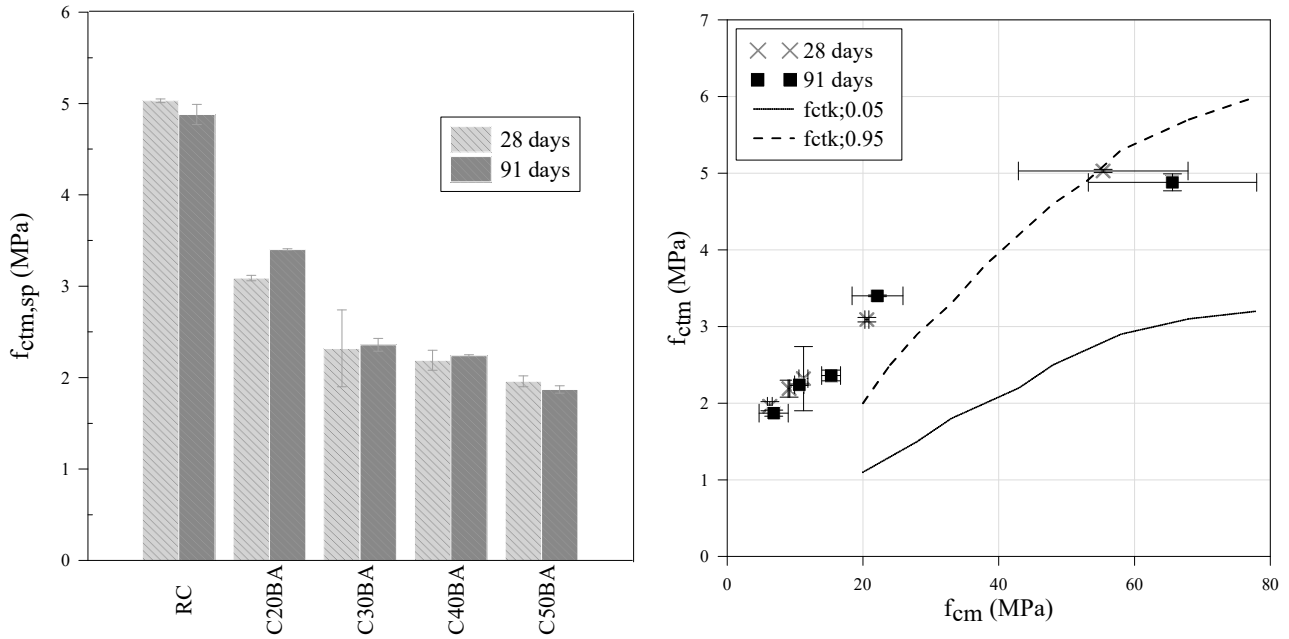

Figure 4. Splitting tensile strength ($f_{ctm,sp}$) vs. replacement level (**left**); relationship between tensile strength (f_{ctm}) and compressive strength in cylindrical specimens (f_{cm}) at 28 and 91 days (**right**).

Table 6 also shows the results of a calculation for the predicted change in splitting tensile strength as a function of the uniaxial compressive strength in cylindrical specimens according to Eurocode 2 [46]. For normal structural uses, the mean tensile strength is related to the cylinder strength using the following equations:

$$f_{ctm} = 0.30 \cdot {f_{ck}}^{2/3}, \text{ for concrete classes } \leq \text{ C50/60} \quad (4)$$

$$f_{ctm} = 2.12 \cdot ln\left(1 + \frac{f_{cm}}{10}\right), \text{ for concrete classes } > \text{ C50/60} \quad (5)$$

The data showed that there is a high correlation between the two parameters, but the measured values of MIBA-containing mixes were higher than expected; both 28-day and 91-day values of these mixes were above the upper limit of the 95% confidence interval. This discrepancy may be due in part to the fact that the standard was developed for conventional concrete and not for SCC and that the corresponding EC2 formulas are meant for mixes with f_{cm} values over 20 MPa, and thus may not be extrapolatable to specimens with lower strength. Additional research is needed on this matter to ascertain the existence of a similar relationship to that of concrete using conventional binders according to EN 197 [13].

3.4.3. Secant Modulus of Elasticity

The secant modulus of elasticity was performed on cylindrical specimens of 150 mm in diameter and 300 mm in height. These specimens were cured in a wet chamber at a temperature of 20 ± 2 °C until testing age according to LNEC E 397 [30]. After curing for 28 days, all mixes containing MIBA had remarkably lower moduli of elasticity as shown in Figure 5 (left). Mixes C20BA, C30BA and C40BA showed a decline of around 47% with respect to the RC, whilst mix C50BA a decrease of more than 70% when compared to the RC. Contrary to expectations, there was a slight decrease in the secant modulus of elasticity from 28 to 91 days. The continuous hydration of cement and pozzolanic reactions of FA and MIBA would be expected to result in the generation of further products of hydration and densification of the microstructure, thereby leading to a higher modulus of elasticity. After 91 days, mixes containing 20%, 30% and 40% MIBA showed a decline of about 52%, whereas the 50% MIBA specimens showed a 78% reduction with respect to the RC. The overall decline in performance is mostly due to the expansion of the concrete throughout its setting period, prompted by the oxidization of Al from MIBA [47,48]. The generation of H_2 gas, which became entrapped within the mix increased the specimens' volume as well as the porosity.

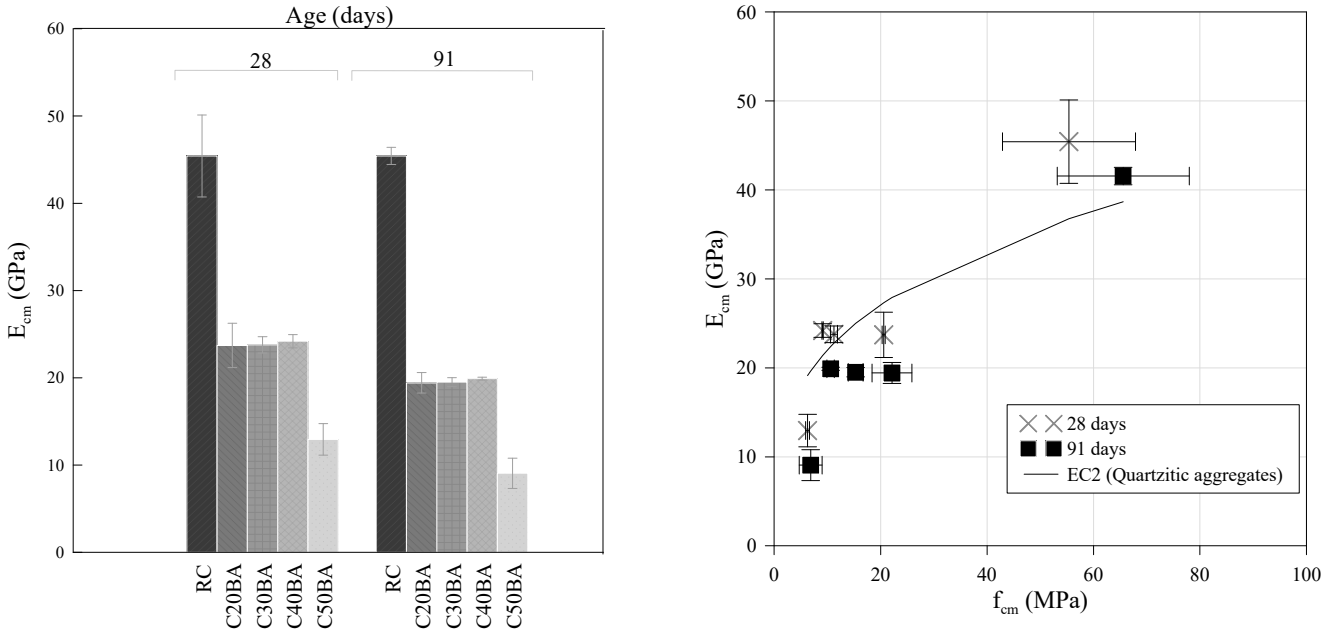

Figure 5. Modulus of elasticity (E_{cm}) at 28 and 91 days (**left**); relationship between E_{cm} and f_{cm} at 28 and 91 days (**right**).

Ravasan [49], when studying concrete containing MIBA as a substitute for fine aggregate (values ranging from 5% to 80%), observed a reduction, albeit less significant, in the modulus of elasticity between these mixtures and the control mix. Pokorný et al. [50] observed a decline in the compressive strength and modulus of elasticity with the use of zinc-rich bottom ash. This metal also presents a similar oxidization reaction when exposed

to OH^- ions in the concrete mix. It is possible that part of the expansion of the specimens in the present study may have been due to the presence of zinc particles in the MIBA.

The curve in Figure 5 (right) represents the theoretical secant modulus of elasticity according to EC2 [39], which has been calculated using Equation (6). These values can be compared with those obtained experimentally as shown in Table 7. Despite the unexpected lower values of the 91-day modulus of elasticity, the relationship between this property and the compressive strength was within expectable ranges.

$$E_{cm} = 22\left(\frac{f_{cm}}{10}\right)^{0.3} \quad (6)$$

Table 7. E_{cm} vs. f_{cm} according to Eurocode 2 [39] at 28 and 91 days.

Mix	$f_{cm,28}$ (MPa)	$E_{cm,28}$ (GPa)		$f_{cm,91}$ (MPa)	$E_{cm,91}$ (GPa)	
		EC2	Measured		EC2	Measured
RC	55.4	36.7	45.4	65.6	38.7	41.6
C20BA	20.8	27.3	23.7	22.1	27.9	19.4
C30BA	11.2	22.8	23.8	15.3	25.0	19.5
C40BA	9.10	21.4	24.2	10.6	22.4	19.9
C50BA	6.28	19.1	12.9	6.85	19.6	9.07

3.4.4. Ultrasonic Pulse Velocity

The ultrasonic pulse velocity (UPV) *versus* curing time for 7, 28 and 91 days is presented in Figure 6. The mixes containing MIBA showed lower, albeit acceptable UPV values, for all ages when compared to the RC. It is noticeable that the UPV changed slightly during the first 28 days. However, an interesting observation is that at 91 days, the RC has presented a UPV of 4918 m/s, which is more than the UPV known for sound concrete (i.e., 4500 m/s [51]).

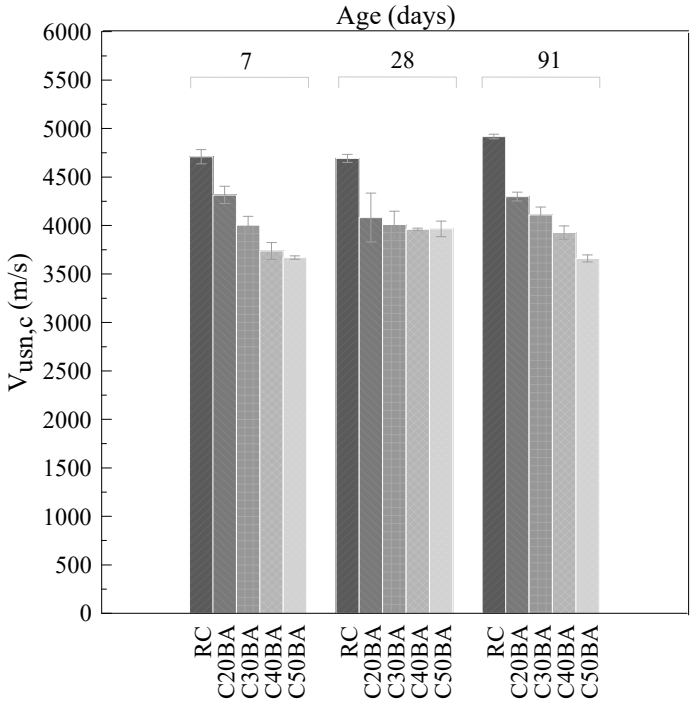

Figure 6. Ultrasonic pulse velocity at 7, 28 and 91 days.

3.4.5. Shrinkage

Figure 7 (left) shows the evolution of shrinkage over 91 days. Simões et al. [14] described the total length of shrinkage in ternary mixes of SCC with FA and MIBA as having rapid initial evolution. In this study, all mixes between 14 to 28 days reached around 50% of their corresponding 91-day shrinkage value. All mixes containing MIBA presented greater shrinkage when compared to the RC and more so with increasing ash content. Other authors witnessed similar results [13,44,53]. Mixes C20BA, C30BA, C40BA and C50BA showed 91-day shrinkage values of ~580 µm/m, ~670 µm/m, ~840 µm/m and ~930 µm/m, respectively, whilst that of the RC was of ~500 µm/m. Up to two–three days after demoulding, mixes C20BA and C30BA presented slight expansion (~100 µm/m), which was then negated with high shrinkage. It is possible that Al particles may have continued to oxidize after setting, thereby prompting an internal expansion of the already hardened specimen.

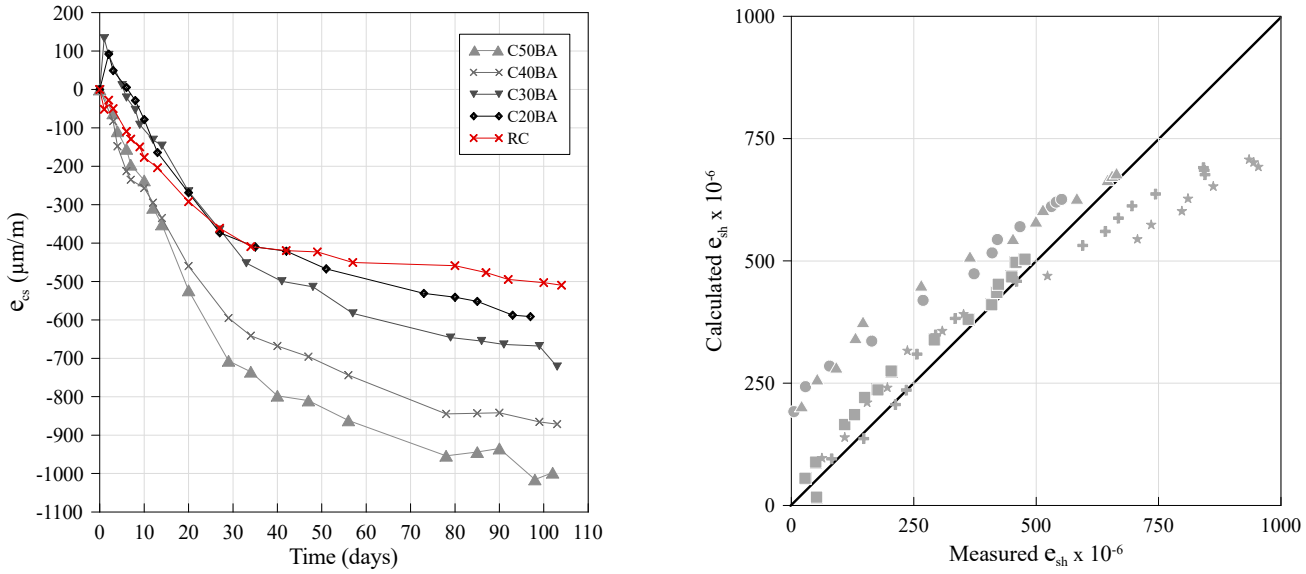

Figure 7. Total shrinkage over 91 days (**left**) and shrinkage calculated according to the Eurocode 2 [46] prediction model (**right**).

Similar behaviour was observed by Cheng [13], having witnessed an accelerated development of shrinkage in the first 28 days, evolving progressively until 91 days. In the same sense, Whittaker et al. [52], when studying the effect of MIBA on the production of mortars, observed an increase in shrinkage in mixes with higher replacement levels. According to the authors, this increase was partly due to the higher w/c ratio that resulted from the ashes' use.

Figure 7 (right) presents the estimate of the total shrinkage values, for conventional concrete, according to the expressions proposed by Eurocode 2 [46], for the ages previously considered. Comparing the calculated vs. measured values, it appears that the EC2 model tends to overestimate shrinkage at early ages. However, over time, shrinkage evolves significantly more in actual specimens, translating into an overlap between the relationship and the line of equality and progressing towards underestimation of the model. After 91 days, RC and C20BA mixes showed an absolute shrinkage value lower than that predicted by EC2, corresponding to approximately 97% and 92%, respectively, of the final value indicated by the standard.

3.5. Durability-Related Performance

3.5.1. Water Absorption by Immersion

Figure 8 shows the results of the water absorption by immersion test at 28 and 91 days. It is clear that the water absorption increased with increasing MIBA content. Nevertheless,

after 28 days, the C20BA mix showed negligible differences when compared to the control concrete with 30% fly ash.

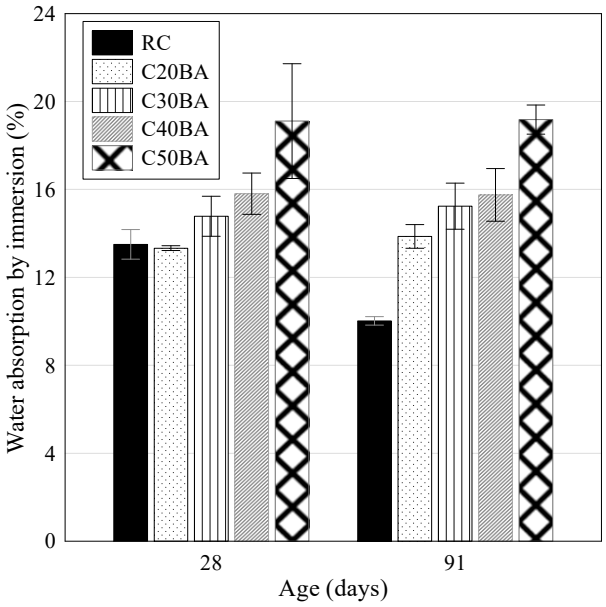

Figure 8. Water absorption by immersion at 28 and 91 days.

Over time, cementitious composites tend to present a porous network with a progressively lower volume accessible to water. Although this was observed for the RC after 91 days, all mixes with MIBA presented little change in this property, thus suggesting little improvement of the microstructure. It is likely that the higher porosity of MIBA mixes was due to the generation of H_2 gas in the fresh state, thus affecting the hardened state performance [50,53]. Furthermore, the little to no improvement over time suggests that the ash presented little pozzolanicity.

3.5.2. Water Absorption by Capillary Action

Table 8 presents the results of the water absorption by capillary action test. A similar development for all mixes was observed throughout the test; the greatest variation in water absorption occurred in the first 6 h where approximately 50% of the final absorption value was attained, but with MIBA-containing mixes exhibiting higher values as the ash's content increased due to the aforementioned reasons; C20BA showed a 16% increase when compared to the RC after 72 h, whereas the C40BA and C50BA showed values over 75%. All mixes showed a reduction in water absorption between 28 and 91 days. This was expected as there is generalized refining of the microstructure with the ensuing generation of products of hydration, leading to greater tortuosity and less interconnectivity of the porous network and thus less water absorption by capillary action. Lin [54] observed similar behaviour when studying vitrified fly ashes from incinerated municipal solid waste as cement replacement (0%, 10%, 20% and 40%).

Table 8. Capillary water absorption results at 28 and 91 days.

Mix	Age (Days)	Water Absorption (kg/m^2)								Capillary Absorption	
		$t_{3\,h}$		$t_{6\,h}$		$t_{24\,h}$		$t_{72\,h}$		Coefficient (mm/min$^{0.5}$)	
		Abs_m	S.D.	Abs_m	S.D.	Abs_m	S.D.	Abs_m	S.D.	$Coef_{abs}$	R^2
RC	28	1.43	0.28	1.83	0.33	2.57	0.46	2.96	0.42	0.095	0.98
	91	0.93	0.20	1.04	0.23	1.34	0.27	1.72	0.39	0.052	0.86
C20BA	28	1.48	0.11	1.87	0.10	2.75	0.24	3.45	0.26	0.095	0.96
	91	0.80	0.23	0.94	0.28	1.34	0.28	1.85	0.29	0.047	0.91
C30BA	28	1.83	0.17	2.40	0.24	3.79	0.44	4.89	0.55	0.125	0.99
	91	0.97	0.04	1.15	0.07	1.68	0.09	2.34	0.23	0.058	0.92
C40BA	28	1.67	0.33	2.23	0.39	3.73	0.60	5.26	0.85	0.116	0.99
	91	0.93	0.11	1.08	0.11	1.51	0.17	2.00	0.17	0.054	0.89
C50BA	28	1.84	0.03	2.45	0.09	3.96	0.20	5.21	0.23	0.126	0.99
	91	1.07	0.12	1.21	0.14	1.70	0.17	2.34	0.20	0.059	0.85

3.5.3. Carbonation

Figure 9 shows the results of the carbonation test, in which the specimens were exposed to an environment with 5% CO_2. The RC showed negligible carbonation and thus was not considered in the figure. Increasing the percentage of MIBA led to an increase in carbonation depth. This outcome was expected from the results of previous tests due to the oxidization reaction of aluminium particles producing gaseous hydrogen, which in turn created a greater porous network facilitating the diffusion of CO_2. Additionally, since the ashes replaced conventional cement, the production of $Ca(OH)_2$ decreased with increasing replacement levels, thereby resulting in a lower amount of material capable of being carbonated and thus accelerated the progression of CO_2. There was an unexpectedly steep increase in carbonation depth for C50BA specimens after 21 days.

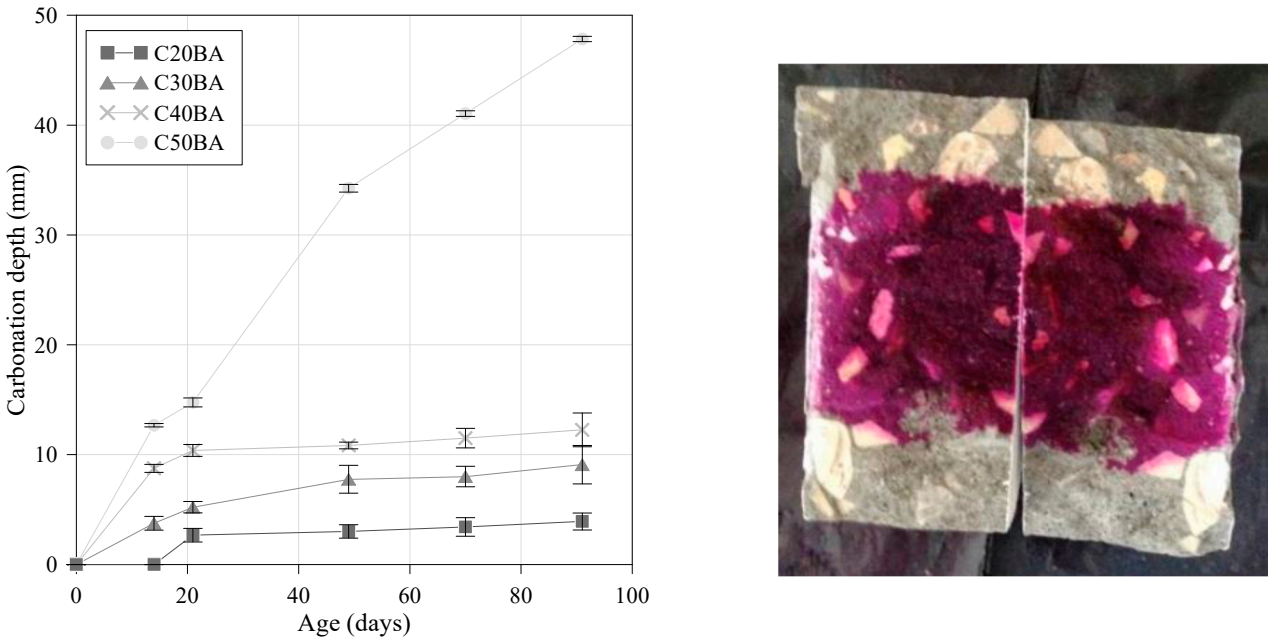

Figure 9. Carbonation depth (**left**) of samples with MIBA (**right**).

3.5.4. Chloride Ion Migration

In Figure 10, the evolution of the chloride diffusion coefficient for 28 and 91 days is shown. As expected, there was a reduction of the chloride diffusion coefficient with increasing age. Increasing the content of MIBA naturally led to higher chloride ion migration coefficients; C20BA, C30BA and C40BA specimens showed values two to three times higher

than those of the RC, whereas those of the C50BA mix were almost four times higher. In the study of Van Der Wegen et al. [55], wherein MIBA was used as aggregate, higher chloride ion penetration had also been observed with increasing replacement level. Conventional fly ash presents pozzolanic activity in the presence of the products of hydration of cement, the result of which decreased the penetration of chloride ions [56]. MIBA, on the other hand, apart from presenting little pozzolanicity, which translates into little additional products of hydration, also led to a greatly porous microstructure, due to the oxidization of aluminium, that facilitated the diffusion of chloride ions.

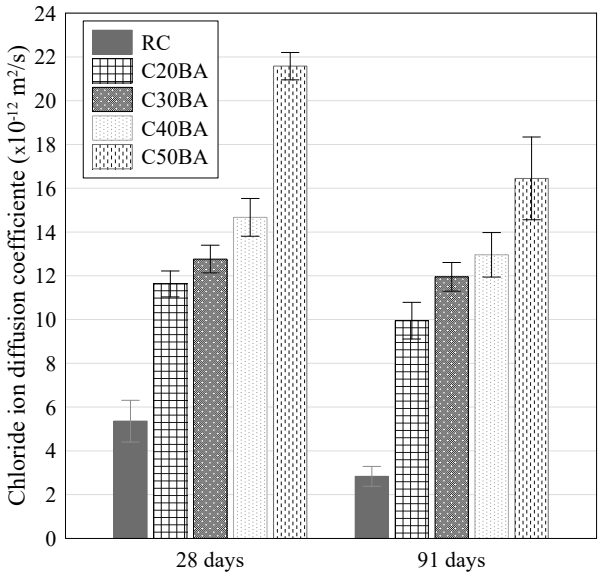

Figure 10. Chloride diffusion coefficient at 28 and 91 days.

3.5.5. Electrical Resistivity

Figure 11 shows the specimens' electrical resistivity over time. As expected from the results of the previous section, electrical resistivity increased for all mixes with increasing age and decreased with increasing replacement of cement. The RC specimens obtained significantly higher values of electrical resistivity, which suggests greater resistance to the penetration of chloride ions and thus delayed corrosion of steel reinforcements. Apart from the RC, the mix that showed the most significant improvement from 28 to 91 days was C50BA, with an improvement of 54%, whereas the others had average variations of ~38%. This infers that the type of addition used has more influence than the replacement level. The same conclusion had been drawn by Silva and de Brito [57,58], where they studied the effect of using limestone filler as cement replacement; increasing the amount of filler led to a reduced increase in electrical resistivity with increasing age (i.e., ~37%). The same authors also produced SCC mixes with fly ash, with replacement levels of 30%, 60% and 70%, having observed an average increase in the electrical resistivity value of 72% from 28 to 91 days, which is comparable to that presented by the RC in this study. It is clear that the use of fly ash, as opposed to limestone filer and MIBA, favours the increase in electrical resistivity. This difference could be due to the fact that the fly ash, unlike limestone filer and MIBA to a lesser extent, shows significant pozzolanic activity, thereby capable of improving the performance of the concrete with age.

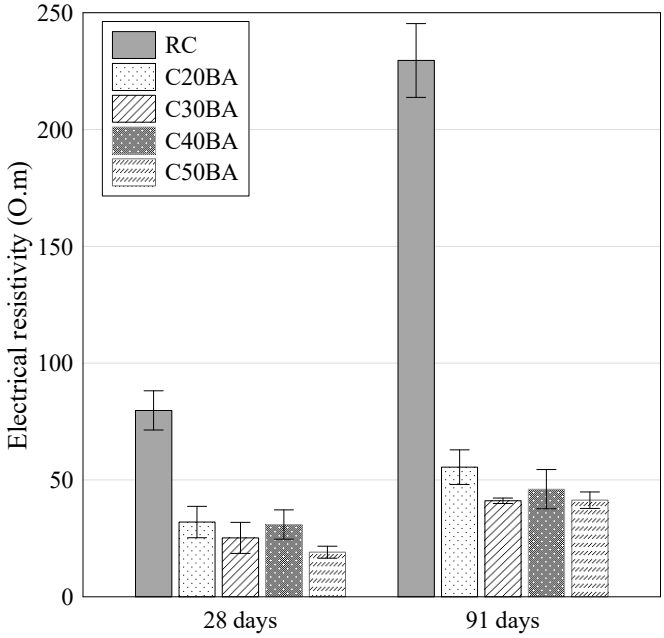

Figure 11. Electrical resistivity coefficient (Ω.m) at 28 and 91 days.

4. Conclusions

This study had the objective of determining the effects of using milled bottom ashes from incinerated municipal solid waste in the performance of self-compacting concrete. It was carried out within the scope of a larger research project aiming to valorise this waste in the production of new construction materials. One other objective of the current study was also to contribute to the wider dissemination of self-compacting concrete and its capacity to incorporate significant amounts of MIBA, leading to greater implementation of this type of concrete in current practice. The conclusions obtained from this study are the following:

- In the slump-flow and V-funnel tests, all mixes presented fluidity, flow rate and viscosity perfectly adjusted to that established in the normative requirements. As for the flow requirements in the L-box test, the mixes C20BA and C50BA presented the worst performance. Even so, the results were deemed as acceptable and, together with the visual analysis carried out during the execution of the test, it is possible to ensure that the produced SCCs present adequate fluidity and flow capacity.
- As for the mechanical performance, the C20BA mixture presents the most favourable overall results of mixes containing MIBA. The rest of the mixtures present considerably higher performance losses, particularly the mixtures C40BA and C50BA, which did not present enough compressive strength for a real structural situation.
- Regarding the durability-related performance, SCCs produced with MIBA present a promising behaviour. The C20BA mixture stood out as the most advantageous mixture with MIBA, presenting values very similar to those of the RC mixture for most of the studied properties. The C50BA mixture, on the other hand, presented the worst behaviour of all the mixtures.

Although the MIBA led to a decline in mechanical properties, evaluating the overall performance of the resulting concrete, as long as the percentage of replacement does not exceed 20%, the MIBA can prove to be promising, since it does not significantly hinder the fresh behaviour of the SCC and represents a new value-added solution for bottom ashes from incinerated municipal solid wastes. Nevertheless, it is recommended that additional research be carried out, especially on the use of pre-treated MIBA in order to eliminate the expansion due to the oxidization of aluminium particles, which is the primary cause for the decline in performance. Assuming that adequate performance levels are attained under these circumstances, MIBA can be considered as an alternative mineral addition capable of partially replacing cement in the production of concrete for several applications

in construction. Furthermore, future research should also focus on an in-depth life cycle assessment, as it is crucial to understand the implications of using MIBA in current practice. It is especially important given the decline in performance when using the addition and what would be the necessary changes in the mix design to consider a functional unit of, for example, one cubic metre of concrete with equivalent mechanical and durability properties in order to carry out an adequate comparative analysis.

Author Contributions: J.R.S. and P.R.d.S. conceived and designed the experiments; J.R.S. performed the experiments; P.R.d.S. and R.V.S. analysed and validated the methodology and results; R.V.S. and P.R.d.S. wrote the paper. All authors have read and agreed to the published version of the manuscript.

Funding: This research was funded by Instituto Politécnico de Lisboa (IPL) through the scientific research project "ECOncrete—Production of self-compacting concrete with municipal solid waste incinerator bottom ash (IPL/2017/ECOnCrete/ISEL)" and FCT- Foundation for Science and Technology through the research project PTDC/ECI- CON/29196/2017 "Recycled Inorganic Polymer Concrete: Towards a fully recycled and cement-free concrete" (RInoPolyCrete).

Institutional Review Board Statement: Not applicable.

Informed Consent Statement: Not applicable.

Data Availability Statement: Not applicable.

Acknowledgments: The authors gratefully acknowledge the support of the CERIS Research Institute, Instituto Superior Técnico of the University of Lisbon and FCT (Foundation for Science and Technology). The authors also acknowledge the contribution of Y. Avila and D. Kassim in the preparation of some figures.

Conflicts of Interest: The authors declare no conflict of interest.

References

1. Lindsey, R. Climate Change: Atmospheric Carbon Dioxide. Available online: https://www.climate.gov/news-features/understanding-climate/climate-change-atmospheric-carbon-dioxide (accessed on 29 June 2021).
2. Department of Trade and Industry. *Our Energy Future—Creating a Low Carbon Economy*; Department of Trade and Industry (DTI): London, UK, 2003; p. 144.
3. Flower, D.J.M.; Sanjayan, J.G. Green house gas emissions due to concrete manufacture. *Int. J. Life Cycle Assess.* **2007**, *12*, 282–288. [CrossRef]
4. Rodgers, L. Climate Change: The Massive CO2 Emitter You May Not Know About. Available online: https://www.bbc.com/news/science-environment-46455844 (accessed on 29 June 2021).
5. Zhang, T.; Gao, P.; Gao, P.; Wei, J.; Yu, Q. Effectiveness of novel and traditional methods to incorporate industrial wastes in cementitious materials—An overview. *Resour. Conserv. Recy.* **2013**, *74*, 134–143. [CrossRef]
6. Jani, Y.; Hogland, W. Waste glass in the production of cement and concrete—A review. *J. Environ. Chem. Eng.* **2014**, *2*, 1767–1775. [CrossRef]
7. Dhir, R.K.; De Brito, J.; Lynn, C.J.; Silva, R.V. *Sustainable Construction Materials: Municipal Incinerator Bottom Ash*; Woodhead Publishing: Duxford, UK, 2018.
8. Hoornweg, D.; Bhada-Tata, P. What a waste: A global review of solid waste management. *Urban. Dev. Ser. Knowl. Pap.* **2012**, *15*, 1–98.
9. DA_58. *Aeiru—Agregados Artificiais de Escórias de Incineração de Resíduos Urbanos para Pavimentos Rodoviários*; Laboratório Nacional de Engenharia Civil (LNEC): Lisboa, Protugal, 2015; p. 8. (In Portuguese)
10. Amat, R.C.; Ismail, K.N.; Noor, N.M.; Ibrahim, N.M. The Effects of Bottom Ash from Mswi Used as Mineral Additions in Concrete. In Proceedings of the MATEC Web of Conferences, EDP Sciences, Ho Chi Minh City, Vietnam, 5–6 August 2016; p. 01053.
11. Jurič, B.; Hanžič, L.; Ilić, R.; Samec, N. Utilization of municipal solid waste bottom ash and recycled aggregate in concrete. *Waste Manag.* **2006**, *26*, 1436–1442. [CrossRef]
12. Lin, K.; Lin, D. Hydration characteristics of municipal solid waste incinerator bottom ash slag as a pozzolanic material for use in cement. *Cem. Concr. Compos.* **2006**, *28*, 817–823. [CrossRef]
13. Cheng, A. Effect of incinerator bottom ash properties on mechanical and pore size of blended cement mortars. *Mater. Des.* **2012**, *36*, 859–864. [CrossRef]
14. Simões, B.; da Silva, P.R.; Silva, R.V.; Avila, Y.; Forero, J.A. Ternary mixes of self-compacting concrete with fly ash and municipal solid waste incinerator bottom ash. *Appl. Sci.* **2021**, *11*, 107. [CrossRef]
15. EN-197-1. *Cement—Part 1: Composition, Specifications and Conformity Criteria for Common Cements*; Comité Européen de Normalisation (CEN): Brussels, Belgium, 2011; p. 50.

16. EN-450-1. *Fly Ash for Concrete. Definition, Specifications and Conformity Criteria*; Comité Européen de Normalisation (CEN): Brussels, Belgium, 2012; p. 34.
17. EN-12620:2002+A1:2008. *Aggregates for Concrete*; Comité Européen de Normalisation (CEN): Brussels, Belgium, 2008; p. 56.
18. EN-1008. *Mixing Water for Concrete—Specification for Sampling, Testing and Assessing the Suitability of Water, Including Water Recovered from Processes in the Concrete Industry, as Mixing Water for Concrete*; Comité Européen de Normalisation (CEN): Brussels, Belgium, 2002; p. 22.
19. EN-934-1. *Admixtures for Concrete, Mortar and Grout. Common Requirements*; Comité Européen de Normalisation (CEN): Brussels, Belgium, 2008; p. 14.
20. EN-934-2. *Admixtures for Concrete, Mortar and Grout. Concrete Admixtures. Definitions, Requirements, Conformity, Marking and Labelling*; Comité Européen de Normalisation (CEN): Brussels, Belgium, 2012; p. 28.
21. Nepomuceno, M.; Oliveira, L.; Lopes, S.M.R. Methodology for mix design of the mortar phase of self-compacting concrete using different mineral additions in binary blends of powders. *Constr. Build. Mater.* **2012**, *26*, 317–326. [CrossRef]
22. Silva, P.; De Brito, J.; Costa, J. Viability of two new mixture design methodologies for self-consolidating concrete. *ACI Mater. J.* **2011**, *108*, 579–588.
23. Ferraz, E.; Andrejkovičová, S.; Hajjaji, W.; Velosa, A.; Santos Silva, A.; Rocha, F. Pozzolanic activity of metakaolins by the french standard of the modified chapelle test: A direct methology. *Acta Geodyn. Geomater.* **2015**, *12*, 289–298. [CrossRef]
24. NBR-15895. *Materiais Pozolânicos—Determinação do teor de Hidróxido de Cálcio Fixado—Método de Chapelle Modificado*; Brazilian Association for Technical Norms (Associação Brasileira de Normas Técnicas—ABNT): Rio de Janeiro, Brasil, 2010; p. 10.
25. EN-12350-8. *Testing Fresh Concrete. Self-Compacting Concrete. Slump-Flow Test*; Comité Européen de Normalisation (CEN): Brussels, Belgium, 2019; p. 14.
26. EN-12350-9. *Testing Fresh Concrete. Self-Compacting Concrete. V-Funnel Test*; Comité Européen de Normalisation (CEN): Brussels, Belgium, 2010; p. 12.
27. EN-12350-10. *Testing Fresh Concrete. Self-Compacting Concrete. L Box Test*; Comité Européen de Normalisation (CEN): Brussels, Belgium, 2010; p. 14.
28. EN-12390-3. *Testing Hardened Concrete—Part 3: Compressive Strength of Test Specimens*; Comité Européen de Normalisation (CEN): Brussels, Belgium, 2009; p. 22.
29. EN-12390-6. *Testing Hardened Concrete—Part 6: Tensile Splitting Strength of Test Specimens*; Comité Européen de Normalisation (CEN): Brussels, Belgium, 2009; p. 14.
30. LNEC-E397. *Concrete: Determination of the Modulus of Elasticity under Compression*; National Laboratory in Civil Engineering (Laboratório Nacional de Engenharia Civil—LNEC): Lisbon, Portugal, 1993; p. 2. (In Portuguese)
31. EN-12504-4. *Testing Concrete. Determination of Ultrasonic Pulse Velocity*; Comité Européen de Normalisation (CEN): Brussels, Belgium, 2004; p. 18.
32. LNEC-E398. *Concrete: Determination of Drying Shrinkage and Expansion*; National Laboratory in Civil Engineering (Laboratório Nacional de Engenharia Civil—LNEC): Lisbon, Portugal, 1993; p. 2. (In Portuguese)
33. LNEC-E391. *Concrete: Determination of Carbonation Resistance*; National Laboratory in Civil Engineering (Laboratório Nacional de Engenharia Civil—LNEC): Lisbon, Portugal, 1993; p. 2. (In Portuguese)
34. LNEC-E394. *Concrete: Determination of Water Absorption by Immersion—Testing at Atmospheric Pressure*; National Laboratory in Civil Engineering (Laboratório Nacional de Engenharia Civil—LNEC): Lisbon, Portugal, 1993; p. 2. (In Portuguese)
35. LNEC-E463. *Concrete: Determination of the Chloride ion Diffusion Coefficient by Non-Steady State Migration*; National Laboratory in Civil Engineering (Laboratório Nacional de Engenharia Civil—LNEC): Lisbon, Portugal, 2004; p. 8. (In Portuguese)
36. Luping, T. *Guidelines for Practical Use of Methods for Testing the Resistance of Concrete to Chloride Ingress*; CHLORTEST—EU Funded Research Project under 5FP GROWTH Programme; Swedich National Testing and Research Institute: Karlskrona, Sweden, 2005; p. 271.
37. Raverdy, M.; Brivot, F.; Paillere, A.M.; Dron, R. Appreciation of pozzolanic reactivity of secondary components. In Proceedings of the 7eme Congres International de la Chimie Des Ciments, Paris, France, 30 June–4 July 1980. (In French).
38. ASTM-C618. *Standard Specification for Coal Fly Ash and Raw or Calcined Natural Pozzolan for Use in Concrete*; American Society for Testing and Materials: West Conshohocken, PA, USA, 2019; p. 5.
39. EN-206:2013+A1:2016. *Concrete—Specification, Performance, Production and Conformity*; Comité Européen de Normalisation (CEN): Brussels, Belgium, 2016; p. 98.
40. Zajac, M.; Rossberg, A.; Le Saout, G.; Lothenbach, B. Influence of limestone and anhydrite on the hydration of portland cements. *Cem. Concr. Compos.* **2014**, *46*, 99–108. [CrossRef]
41. Kim, J.; An, J.; Nam, B.H.; Tasneem, K.M. Investigation on the side effects of municipal solid waste incineration ashes when used as mineral addition in cement-based material. *Road Mater. Pavement Des.* **2016**, *17*, 345–364. [CrossRef]
42. Lynn, C.J.; Dhir, R.K.; Ghataora, G.S. Municipal incinerated bottom ash use as a cement component in concrete. *Mag. Concr. Res.* **2017**, *69*, 512–525. [CrossRef]
43. Loginova, E.; Schollbach, K.; Proskurnin, M.; Brouwers, H.J.H. Municipal solid waste incineration bottom ash fines: Transformation into a minor additional constituent for cements. *Resour. Conserv. Recycl.* **2021**, *166*, 105354. [CrossRef]
44. Pera, J.; Coutaz, L.; Ambroise, J.; Chababbet, M. Use of incinerator bottom ash in concrete. *Cem. Concr. Res.* **1997**, *27*, 1–5. [CrossRef]

45. Li, X.-G.; Lv, Y.; Ma, B.-G.; Chen, Q.-B.; Yin, X.-B.; Jian, S.-W. Utilization of municipal solid waste incineration bottom ash in blended cement. *J. Clean. Prod.* **2012**, *32*, 96–100. [CrossRef]
46. EN-1992-1-1:2004+A1:2014. *Eurocode 2—Design of Concrete Structures: Part 1-1: General Rules and Rules for Buildings*; Comité Européen de Normalisation (CEN): Brussels, Belgium, 2014; p. 259.
47. Dwivedi, A.; Jain, M.K. Fly ash—Waste management and overview: A review. *Recent Res. Sci. Technol.* **2014**, *6*, 30–35.
48. Bertolini, L.; Carsana, M.; Cassago, D.; Curzio, A.Q.; Collepardi, M. Mswi ashes as mineral additions in concrete. *Cem. Concr. Res.* **2004**, *34*, 1899–1906. [CrossRef]
49. Ravasan, F.M. Characterization and mechanical properties of concrete mixtures made with sedimentary lime and industrial incinerator ash. *Malays. J. Civ. Eng.* **2014**, *26*, 1–18.
50. Pokorný, P.; Dobiáš, D.; Čítek, D. The influence of corrosion of zinc powder on mechanical properties of concrete. *Ceram. Silikáty* **2016**, *60*, 195–199. [CrossRef]
51. Breysse, D. *Non-Destructive Assessment of Concrete Structures: Reliability and Limits of Single and Combined Techniques: State-Of-The-Art Report of the Rilem Technical Committee 207-Inr*; Springer Science & Business Media: Amsterdam, The Netherlands, 2012; p. 374.
52. Whittaker, M.; Taylor, R.; Li, S.; Li, Q.; Black, L. The behaviour of finely ground bottom ash in portland cement. In Proceedings of the 29th Cement and Concrete Science Conference, Leeds, UK, 7–8 September 2009; pp. 70–73.
53. Nithiya, A.; Saffarzadeh, A.; Shimaoka, T. Hydrogen gas generation from metal aluminum-water interaction in municipal solid waste incineration (mswi) bottom ash. *Waste Manag.* **2018**, *73*, 342–350. [CrossRef]
54. Lin, K.L. The influence of municipal solid waste incinerator fly ash slag blended in cement pastes. *Cem. Concr. Res.* **2005**, *35*, 979–986. [CrossRef]
55. Van Der Wegen, G.; Hofstra, U.; Speerstra, J. Upgraded mswi bottom ash as aggregate in concrete. *Waste Biomass Valori.* **2013**, *4*, 737–743. [CrossRef]
56. Chinthakunta, R.; Ravella, D.P.; Sri Rama Chand, M.; Janardhan Yadav, M. Performance evaluation of self-compacting concrete containing fly ash, silica fume and nano titanium oxide. *Mater. Today: Proc.* **2021**, *43*, 2348–2354.
57. Silva, P.; de Brito, J. Experimental study of the mechanical properties and shrinkage of self-compacting concrete with binary and ternary mixes of fly ash and limestone filler. *Eur. J. Environ. Civ. Eng.* **2017**, *21*, 430–453. [CrossRef]
58. da Silva, P.R.; de Brito, J. Durability performance of self-compacting concrete (scc) with binary and ternary mixes of fly ash and limestone filler. *Mater. Struct.* **2016**, *49*, 2749–2766. [CrossRef]